How to resolve HTI effects from marine narrow-azimuth data?

Nizare El Yadari, Richard Winnett, Kelly Beauglehole, Thomas Hertweck (Fugro Seismic Imaging Ltd.)

This paper was prepared for presentation during the 12th International Congress of the Brazilian Geophysical Society held in Rio de Janeiro, Brazil, August 15-18, 2011.

Abstract

Media exhibiting horizontal transverse isotropy (HTI) are usually associated with an oriented stress field or open fractures. Seismic reflection traveltimes beneath such media vary with the source-receiver azimuth. Firstly, we present a P-wave seismic processing method which simultaneously scans for three characteristic HTI parameters to optimize the moveout correction of narrow azimuth (NAZ) CMP gathers, where multi-azimuth (MAZ) techniques like sectoring are unsuitable. Secondly, we extend the method to detect the fracture direction and to run the automatic analysis on 3D super-gathers. Finally, we apply to a marine multi-source/streamer NAZ data demonstrates the effectiveness of this method.

Introduction

The estimation of subsurface properties forms a major part of seismic processing. Combining these properties with increasingly complex physical models we attempt to compensate for the distortions in the recorded data. Detecting and compensating for anisotropy removes further distortions and reveals more detail about the state of the subsurface like stress and fracturing. Conventionally, this process starts in the time domain with CMP gathers and the manual estimation of velocity to optimize the kinematic adjustment by normal move-out correction. The horizontal layering assumption and the resolution of seismic data limits our model space and we may focus on parameterizations which flatten gathers assuming their gradual changes remain spatially and geologically consistent. When anomalies occur we test for measurement errors or contamination by non-reflection energy before increasing the complexity of our physical models to deal with it. Azimuthal anisotropic effects are one such challenge.

Availability of MAZ data increases the likelihood of encountering kinematic effects that display azimuthal dependence. NAZ multi-source and streamer geometries and long cables are not immune to this either. Azimuth-sorted CMP gathers in areas where azimuthal anisotropy is present (e.g., caused by vertical fractures) exhibit short period ripples in residual Δt after a normal moveout correction. Incorporating the effect of anisotropy during seismic processing and estimating anisotropic parameters is an active area of research. In general, extending anisotropic parameter determination beyond the vertical transverse isotropy (VTI) case is a serious challenge. Which model should we use (tilted, structural, HTI or orthorhombic) and how do we resolve all their corresponding parameters?

Whether time or depth imaging, the initial automatic analysis is performed in the un-migrated time-midpoint domain. An azimuthally anisotropic moveout correction can be applied to remove most of the HTI 2nd and 4th order moveout effects. Isotropic inverse moveout may then be performed to allow a purely isotropic approach for the subsequent processing steps. Any anisotropic parameters learned at this stage can form the basis for starting models for tomography, PSDM, and interpretation. Assisted by a new formulation of the analytical reflection traveltime equation and a coherency-based measure within the automatic analysis, we can resolve HTI problems even in NAZ data without the need for ellipse fitting (Al-Dajani et al., 2001). The method is valid for NAZ as well as MAZ surveys (El Yadari et al., 2010).

Our approach exploits the anisotropic P-wave traveltime equation for horizontal layers (Al-Dajani and Tsvankin, 1998) with a modification for convenient representation of the reference subsurface fields and their azimuth dependency. To better understand how the HTI effect can be removed properly, we will firstly show an application of the method to CMP gathers from an area where the dominant fracturing direction (i.e., the axis of symmetry orientation) is known. Then, we will extend the method to estimate fracture orientation and make use of 3-D super-gathers to ensure more stability.

Method

A system of parallel vertical fractures embedded in an isotropic medium exhibits HTI behavior. By analogy, tilting the VTI symmetry axis to horizontal leads to the HTI model. Hence, HTI is the simplest possible model of a formation with vertical fractures. P-wave reflection traveltimes in HTI media are conveniently expressed in terms of δ and η as suggested by Tsvankin (2001), where, δ and η are the anisotropic parameters in the vertical plane containing the axis of symmetry. By analogy with the VTI case, δ is defined from the stiffness coefficients simplified by Thomsen's parameterization (Thomsen, 1986) and η is the anellipticity coefficient introduced by Alkhalifah and Tsvankin (1995). Thus, the VTI equation originally developed by Alkhalifah and Tsvankin (1995) can be extended to express long spread P-wave HTI moveout for any source-receiver azimuth (β) and offset X as:

$$T^2(X,\alpha) = T_0^2 + \frac{X^2}{V_{nmo}^2(\alpha)} + \frac{2\eta(\alpha)X^4}{V_{nmo}^2(\alpha)[T_0^2 V_{nmo}^2(\alpha) + 2\eta(\alpha)X^2]}.$$

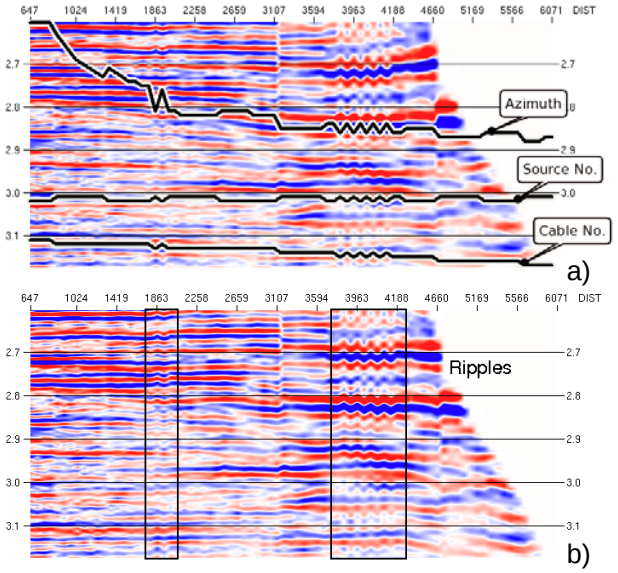

Fig 1: *Isotropic conventional NMO corrections with a) 2nd order and b) 4th order. Acquisition geometry variations correlate with residual anisotropic moveout, as highlighted.*

Here, T_0 is the zero-offset time, $V_{nmo}(\alpha)$ is the azimuthally varying NMO velocity (i.e., the NMO ellipse), and $\eta(\alpha)$ is the azimuthally varying anellipticity coefficient. The parameter $\alpha = \varphi - \beta$, is the angle between the NMO ellipse orientation (i.e., the axis of symmetry), denoted by φ, and the source-to-receiver orientation, denoted by β. For the sake of practicality, we have modified $V_{nmo}(\alpha)$ and $\eta(\alpha)$ to be expressed in terms of any dominant source-receiver azimuth β_0, reference NMO velocity and reference η, denoted by V_0 and η_0 respectively, as follows:

$$V_{nmo}^2(\alpha) = \frac{1 + 2\delta \cos^2(\alpha_0 - \varphi)}{1 + 2\delta \cos^2(\alpha - \varphi)} V_0^2 ,$$

and

$$\eta(\alpha) = \frac{N(\alpha, \alpha_0)}{N(\alpha_0, \alpha_0)} \eta_0 .$$

The above equations show a way of determining subsurface properties for HTI media. It is obvious that this will require an automatic estimation method to resolve the four parameters V_0, φ, δ, and η_0. Selection of those four parameters at any one event and CMP location is extremely difficult and liable to human error or bias. The optimum set of parameters varies from sample to sample over a wavelet length, making it difficult even to select the optimum time pick. The geophysicist cannot perceive the multidimensional trends from the data alone. Especially when the azimuthal coverage is poor (e.g., NAZ), an automatic approach is required.

In principle, automatic picking uses a coherence measure to fit the moveout curves to the recorded reflection events. The data in each CMP gather are tested for alignment with a set of reflection traveltime curves T(X,α).

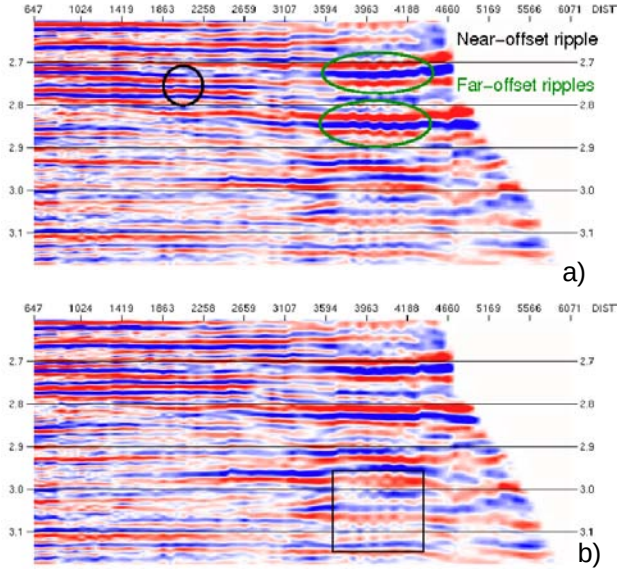

Fig. 2: *Azimuthal NMO corrections using HTI model. (a) HTI2 NMO correction using an automatically scanned, time variant δ function. (b) 4th order with time variant δ and η reduces the ripples.*

Each curve is parameterized by a zero offset time T_0, V_0, φ, δ, and η_0 according to the HTI moveout equation. Each curve defines a summation trajectory over offset and azimuth. The greater the power of the sum, the better the alignment along that curve. Thus, by sweeping through a range of T_0, V_0, φ, δ, and η_0, we transform the data in CMP(X,T) to coherence (V_0, φ, δ, η_0, T_0). The next step locates significant peaks within the multi-dimensional coherence hyper-volume. The four parameters V_0, φ, δ, and η_0 associated with each peak at the T_0 of interest are tested for consistency against a priori constraints. Velocity constraints are obtained by interactive picking at sparse CMP locations of reference source-receiver azimuth (β_0) throughout the survey volume, and used as a guide for the automated picking process. Likewise, fracture direction and anisotropic parameter ranges are manually chosen with respect to the velocity field associated with the same reference azimuth (β_0). Note, it is not possible for example to cascade a series of 1-D searches of V_0 followed by φ then δ because the apparent velocity changes with azimuth. This is already a challenge for 2nd order moveout fitting. Therefore, V_0, φ, and δ must be resolved together as suggested by the NMO ellipse equation. Hereafter, we refer to this step as picking HTI2 parameters. Similarly, HTI4 refers to the process of picking parameters for the 4th order relationship in offset. The picking process certainly appears to require a global search in three parameters for HTI2 and four parameters for HTI4.

Marine NAZ CMP gathers

We apply our method to marine NAZ CMP gathers recorded from offshore Australia. The gathers are comprised of mixed source-cable traces due to the acquisition feathering. Figure 1a shows a gather corrected with 2nd order isotropic NMO. We notice that even adjacent offset traces manifest residual moveout

artifacts. The ripples correlate with the variations in source-receiver azimuth as annotated on the display. The application of 4th order isotropic moveout correction reduces the 'hockey-stick' residual moveout (figure 1b). However, isotropic moveout correction cannot compensate for the short-period ripples. The resultant stack reveals short period pull-up/push-down artifacts.

To assist our anisotropic moveout analysis, previous study provided initial guidance about the orientation of fracturing ($\varphi = 135°$) and constant eccentricity ($\delta = 0.1$) of the regional azimuthal velocity anomaly. As a first step, a manual sweep of different constant values of δ (i.e., eccentricity) showed promising results and confirmed the orientation of the axis of symmetry, but a continuous automatic scan was required to resolve the time-variant behavior of δ. For simplicity, φ was initially assumed constant and known. It is associated with a regional stress direction in this area. Using initial velocity constraints derived from an automatic isotropic high-order moveout scan (see figure 1b), the RMS velocity was allowed to vary within a corridor of ±10%, and the corresponding interval velocity (inverted using the Dix equation) to within ±35%. δ was merely constrained with a fixed range of ±0.2 to perform HTI2 analysis. Figure 2a shows the result of applying 2nd order HTI-type NMO with V_0 and δ derived from the automated scan. The gather is now flatter than the 4th order isotropic NMO correction, but some small ripples remain mainly in the far offset data.

The presence of residual moveout in the far offsets suggests that a higher-order HTI solution may be appropriate. Therefore, an additional simultaneous scan of V_0, δ, and η_0 over the range ±0.3 has been performed. Figure 2b is the same gather now corrected with the optimum HTI4 solution. This last scan has further refined V_0 and δ values to improve the near-offset ripple. As expected, the additional 4th order term in η_0 has resolved most of the ripples in the far-offset traces, removed the kink around offset 3107m, and flattened the regions highlighted in figure 2a. There are still small fluctuations in the far offset traces. This may be due to the horizontal NMO assumption and/or the use of just an HTI model. A more realistic anisotropic model (e.g., orthorhombic) should be more appropriate. Also, the top of the boxed area in figure 2b shows a distinct undulation which is more exaggerated by HTI4 than HTI2.

To investigate this undulation, we extracted sub-sets from the four-dimensional T_0-V_0-δ-η_0 coherence volume itself. Note, the automatic scan picks the peak trend from this volume within the constraint corridor from the auto-picked isotropic velocity profile. Thresholds of the coherence values are used to isolate peaks associated with each major event. As it is difficult to display multi-dimensional volumes, we show sub-sets from the coherence hyper-volume at surfaces extracted along the optimum V_0-δ-η_0 trend. These are displayed separately in figure 3 from left to right as V_0 versus time and similarly for δ and η_0. For simplicity the values of the anisotropic parameters δ and η_0 have been scaled by 1000. There is a good correlation between the times at which V_0, δ and η_0 coherence maxima are observed down to 2.8s, and note the time-variant behavior of δ and η_0. The picked δ is in general agreement with the typical regional value as initially provided. In the case of the undulating event, the coherence character is too broad and indistinct, resulting in a poorly picked η_0 value (see figure 3 near 3.0s). Actually, this event is flatter with the HTI2 correction in figure 2a. A cascaded search may beneficially replace the global search, i.e., one which exploits the constraints imposed from picking HTI2 parameters, then perturbing these slightly while picking η_0. This is similar to the work of Vasconcelos and Tsvankin (2006) who developed a three step procedure to search for multiple parameters in WAZ surveys more efficiently.

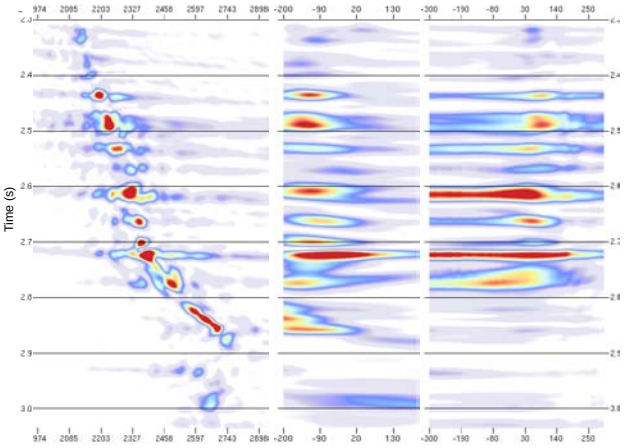

Fig. 3: *Coherence panels from the 4D volume: V_0, δ and η_0 versus time, from left to right.*

Fracture direction detection

Previously, we showed that azimuthal-anisotropic moveout parameters could be determined by simultaneous constrained scanning using a coherence measure. This was quite successful given a-priori knowledge of the dominant stress direction, for this particular dataset where $\varphi = 45°$. In general, φ is space variant. Then, a-priori information from well logs is not adequate. Therefore, we extended our methodology to estimate φ as well. To test the regional anisotropic guidance, we scanned for the same range of HTI2 parameters but with variable φ over a range of ± 90°, with an increment of 5°. Figure 4a shows the resultant coherency extracted from the 4D coherence (V_0, φ, δ, T_0) hyper-volume along surfaces of optimum parameter trends for each φ. Figure 4b shows a similar result but after an HTI4 parameter analysis, where the method delivers better focussed coherence because the events are optimally aligned, offering greater sensitivity to φ estimation. Notice that the HTI2 scan is adequate to detect the fracture direction.

Here we only display regions of significant coherence variation, as a function of varying φ. These coincide with the expectations of the anisotropy in this area. Note, such a technique could be used as the main criterion for detecting azimuthal anisotropic zones elsewhere. Also, the coherency variation exhibits a symmetrical behaviour with two highs separated by approximately 90°. These can be explained in terms of the NMO ellipse. Actually, V_φ and V_0 represent the apparent velocity along the axis of symmetry and orthogonal to it, respectively.

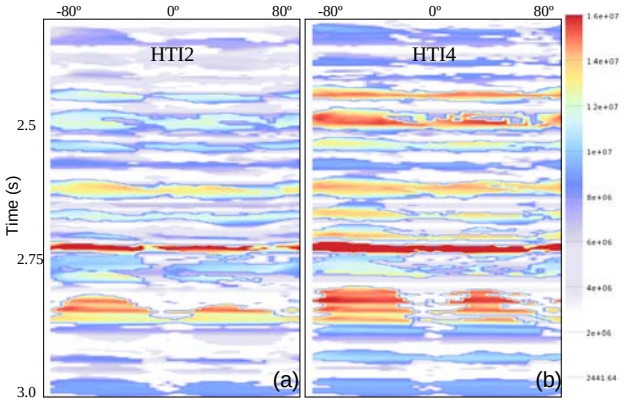

Fig. 4: *Coherence hyper-volume slices as a function of varying φ.*

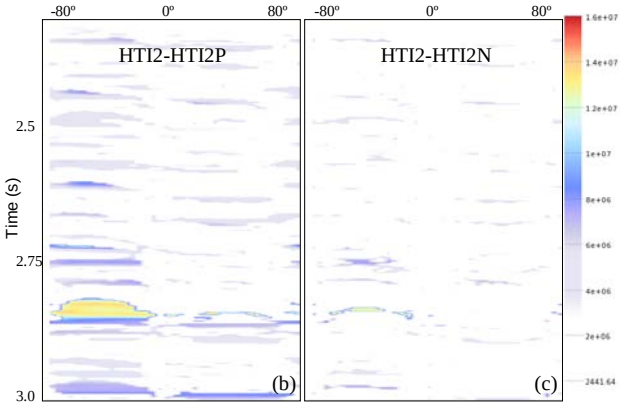

Fig. 5: *Coherence hyper-volume residuals as a function of varying φ.*

V_φ and V_0 lie on the semi-major and semi-minor axes of the ellipse. δ is related to the elliptical eccentricity by: $V_\varphi = V_0 \sqrt{(1+2\delta)}$. Changing the orientation of the ellipse by 90° implies interchanging V_φ with V_0, which is equivalent to changing the sign of δ. In principle, the complexity of the Earth rarely fits the HTI representation, which explains why we do not see exact symmetry in our results. The maximum of the two coherence highs suggests that φ should be -50°, rather than 45° as advised. This dilemma emphasizes the need for a-priori information concerning the sign of δ, but not necessarily its magnitude. When there is no a-priori information, the lack of symmetry noted above offers a mechanism to determine the correct sign. We perform two additional constrained scans denoted by HTI2N and HTI2P in figure 5 corresponding to just negative and positive δ, respectively. Figure 5 illustrates the residuals between the full range and each of the constrained ranges. We conclude that δ is likely to be positive because the corresponding residual coherence is minimized in the zone of positive φ, indicating that φ is 45° as suggested from previous studies. Deriving the spatial variation of φ using a full HTI4 scan would be too costly. We have already shown that HTI2 is adequate. However, a sensitivity analysis indicated that the cost can be reduced further by taking a cascaded scan approach, as mention in the previous section.

Marine NAZ 3D super-gathers

We have already demonstrated that an HTI effect can be detected and compensated even within NAZ CMP gathers. Remember, the HTI effect manifests itself as a residual moveout, referred to as a ripple. Therefore, the key to success in HTI analysis is ensuring the existence of adequate ripple effects. We do this by increasing the azimuthal content. This can easily be performed by expanding the analysis to include traces from adjacent 3D cross-lines, which tend to contain additional azimuths from alternative source-streamer geometries. This approach is often referred to as creating 3D super-gathers. Figure 6 and 7 show comparisons of gathers before and after HTI moveout correction applied to traces from 3D super-gathers formed from 3 adjacent cross-lines. In figure6, the moveout correction has been applied.

The gathers in figure 7 are displayed after HTI compensation, with a 2nd order correction on the top of each figure and 4th order on the bottom. The trace geometry composition, azimuth, source and cable number is annotated on figure 6. As expected, the super-gather selection includes more variations of azimuth due to the additional source and streamer combination. Note, the gradation of streamer content from near to far offset traces is caused by feathering. The resultant increase in azimuthal variation as well as in azimuthal residual moveout anomalies is evident from the characteristic ripples between the seismic traces. After high-order isotropic moveout correction the overall alignment is improved but again the unresolved short-period ripple is exaggerated and widespread compared to the result obtained with CMP gather. The low inter-trace coherency measure increases the sensitivity of our method, allowing it to easily converge to the optimum parameters. The HTI2 correction reduces the ripples in the near offsets as expected, but residual ripples remain in the far offsets where the role of a high-order correction is more dominant. Consequently, the HTI4 solution both improves the alignment out to far offsets and tackles the ripple effect in general. However, other anomalies remain. We suspect these are not resolved properly due to the horizontally layered HTI model assumption, and to the lack of any structural compensation to the 3D super-gather data. The use of a more realistic orthorhombic model or a migration-based implementation would be more appropriate, but also much more costly. Nevertheless, our approach can provide good initial parameters to a more sophisticated inversion scheme. The optimized gather displayed in figures 2b and 7b suggests that this method should minimize structural anomalies, offering two possible options for further processing: The potential to continue processing using an isotropic approach by applying an anisotropic moveout followed by an inverse isotropic moveout. Or the anisotropic parameters may be used as initial parameters for depth imaging.

Figure 8 compares the isotropic versus HTI2 corrected stack results from the same cross-line. The overlay curves detail the predominant sail-line, and azimuthal content pre-stack. The isotropic stack shows anomalous breaks in event continuity.

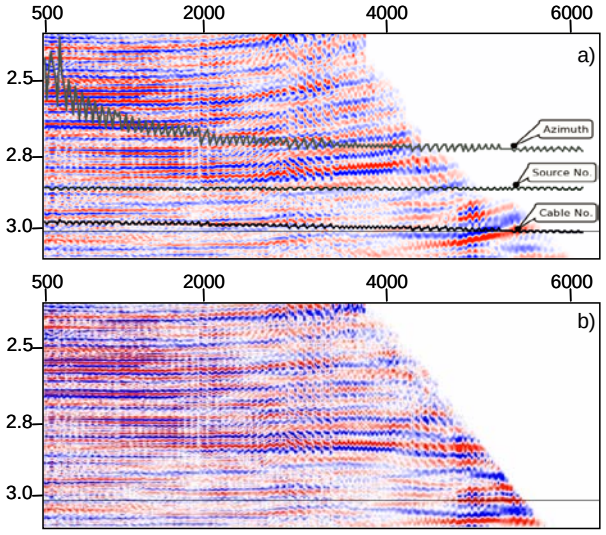

Fig 6: *Isotropic NMO with 2nd (a) and 4th (b) order.*

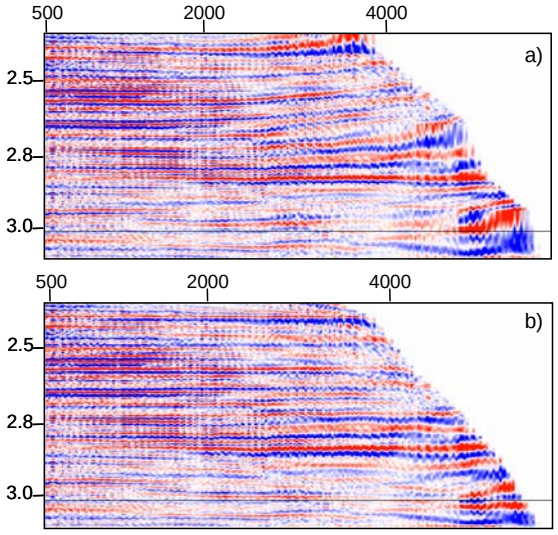

Fig 7: *HTI corrections with 2nd (a) and 4th (b) order.*

These breaks largely disappear after the HTI correction is applied. As suspected, the structure contains dipping horizons which may have contributed to the residuals noticed in the super gathers. Nevertheless, even in the presence of dip, the improved stack continuity highlights the merits of this simple approach.

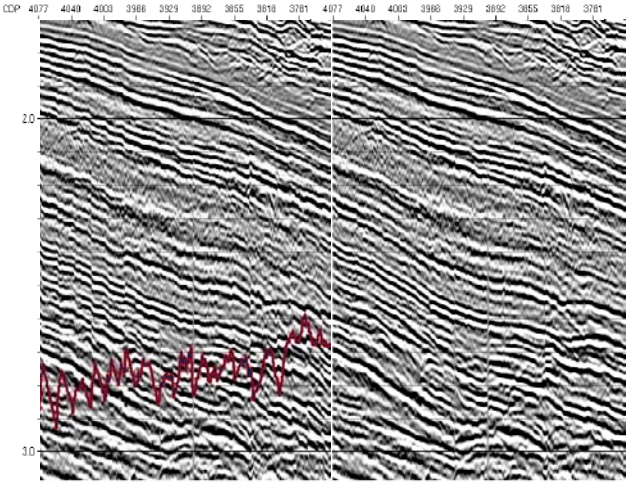

Fig. 8: *4th order NMO (left) versus 2nd order HTI (right) corrected stacks from the same cross-line. The overlay curve illustrates mean azimuth, and the displayed values range from 74º to 108º.*

Conclusions

We have presented an automated fracture detection, velocity and anisotropic parameter estimation method. The method is valid for NAZ as well as WAZ surveys. The approach follows the well-known anisotropic P-wave traveltime equation but modified for convenient representation of the reference subsurface fields and their azimuth dependency. A 2nd order HTI solution was shown to be sufficient to determine the fracture direction. The flatter gathers demonstrated the need for a high-order HTI approach. The sensitivity of the method to the residual HTI effect has been enhanced by the use of 3D super-gathers. The method has been applied to a NAZ dataset in an area with known anisotropic anomalies. The estimated parameters agree with typical values for the region, and stacked sections are improved. The current method is based on the HTI assumption, but can be extended to more realistic models such as the orthorhombic case.

Acknowledgments

The authors would like to thank Fugro for access to seismic data and permission to present this work.

References

Al-Dajani, A., T. Alkhalifah, and F. Morgan, 2001, Reflection moveout inversion in azimuthally anisotropic media: accuracy, limitations and acquisition: Geophysical Prospecting, **47**, 735–756.

Al-Dajani, A., and I. Tsvankin, 1998, Nonhyperbolic reflection moveout for horizontal transverse isotropy: Geophysics, **63**, 1738–1753.

El Yadari, N., Winnett R., Hertweck T., and Beauglehole K., Automatic velocity and anisotropic parameter analysis for HTI media: Application to marine narrow-azimuth data, Expanded Abstract, Denver 2010, USA, 80th Annual Meeting, SEG.

Thomsen, L., 1986, Weak elastic anisotropy: Geophysics, **51**,1954–1966.

Tsvankin, I., 2001, Seismic signatures and analysis of reflection data in anisotropic media: Elsevier.

Vasconcelos, I., and I. Tsvankin, 2006, Nonhyperbolic moveout inversion of wide-azimuth P-wave data for orthorhombic media: Geophys. Prosp., **54**.